Video Article

Fabrication of Three-Dimensional Graphene-Based Polyhedrons *via* Origami-Like Self-Folding

Daeha Joung[1], Daniel Wratkowski[1], Chunhui Dai[1], Seokhyeong Lee[1], Jeong-Hyun Cho[1]

[1]Department of Electrical and Computer Engineering, University of Minnesota, Minneapolis, United States

Correspondence to: Jeong-Hyun Cho at jcho@umn.edu

URL: https://www.jove.com/video/58500
DOI: doi:10.3791/58500

Keywords: Engineering, Issue 139, graphene, graphene oxide, 3D graphene-based cubes, microcubes, self-folding, origami

Date Published: 9/23/2018

Citation: Joung, D., Wratkowski, D., Dai, C., Lee, S., Cho, J.H. Fabrication of Three-Dimensional Graphene-Based Polyhedrons *via* Origami-Like Self-Folding. *J. Vis. Exp.* (139), e58500, doi:10.3791/58500 (2018).

Abstract

The assembly of two-dimensional (2D) graphene into three-dimensional (3D) polyhedral structures while preserving the graphene's excellent inherent properties has been of great interest for the development of novel device applications. Here, fabrication of 3D, microscale, hollow polyhedrons (cubes) consisting of a few layers of 2D graphene or graphene oxide sheets *via* an origami-like self-folding process is described. This method involves the use of polymer frames and hinges, and aluminum oxide/chromium protection layers that reduce tensile, spatial, and surface tension stresses on the graphene-based membranes when the 2D nets are transformed into 3D cubes. The process offers control of the size and shape of the structures as well as parallel production. In addition, this approach allows the creation of surface modifications by metal patterning on each face of the 3D cubes. Raman spectroscopy studies show the method allows the preservation of the intrinsic properties of the graphene-based membranes, demonstrating the robustness of our method.

Video Link

The video component of this article can be found at https://www.jove.com/video/58500/

Introduction

Two-dimensional (2D) graphene sheets possess extraordinary optical, electronic, and mechanical properties, making them model systems for the observation of novel quantum phenomena for next-generation electronic, optoelectronic, electrochemical, electromechanical, and biomedical applications[1,2,3,4,5,6]. Apart from the as-produced 2D layered structure of graphene, recently, various modification approaches have been investigated to observe new functionalities of graphene and seek new application opportunities. For example, modulating (or tuning) its physical properties (*i.e.,* doping level and/or band gap) by tailoring the shapes or patterning of the 2D structure to a one-dimensional (1D) or zero-dimensional (0D) structure (*e.g.*, graphene nanoribbon or graphene quantum dots) has been studied to obtain new physical phenomena including quantum confinement effects, localized plasmonic modes, localized electron distribution, and spin-polarized edge states[7,8,9,10,11,12]. In addition, varying the texture of 2D graphene by crumpling (often called kirigami), delamination, buckling, twisting, or stacking of multiple layers, or changing the graphene surface shape by transferring 2D graphene on top of a 3D feature (substrate) has been shown to change the graphene's wettability, mechanical characteristics, and optical properties[13,14].

Beyond changing the surface morphology and layered structure of 2D graphene, assembly of 2D graphene into functionalized, well-defined, three-dimensional (3D) polyhedrons has been of great interest recently in the graphene community to obtain new physical and chemical phenomena[15]. In theory, the elastic, electrostatic, and van der Waals energies of 2D graphene-based structures can be leveraged to transform the 2D graphene into various 3D graphene-origami configurations[16,17]. Based on this concept, theoretical modeling studies have investigated 3D graphene structure designs, formed from nanoscale 2D graphene membranes, with possible uses in drug delivery and general molecular storage[16,17]. Yet, the experimental progress of this approach is still far from realizing these applications. On the other hand, a number of chemical synthetic methods have been developed to achieve 3D structures *via* template-assisted assembly, flow-directed assembly, leavening assembly, and conformal growth methods[18,19,20,21,22]. However, these methods are currently limited in that they cannot produce a 3D, hollow, enclosed structure without losing the intrinsic properties of the graphene sheets.

Here, a strategy for building 3D, hollow, graphene-based microcubes (overall dimension of ~200 µm) by using origami-like self-folding is outlined; overcoming the foremost challenges in the construction of free-standing, hollow, 3D, polyhedral, graphene-based materials. In origami-like, hands-free self-folding techniques, 2D lithographically patterned planar features (*i.e.,* graphene-based membranes) are connected with hinges (*i.e.,* thermal-sensitive polymer, photoresist) at various joints, thereby forming 2D nets which fold up when the hinges are heated to melting temperature[23,24,25,26]. The graphene-based cubes are realized with window membrane components composed of a few layers of chemical vapor deposition (CVD) grown graphene or graphene oxide (GO) membranes; both with the use of polymer frames and hinges. The fabrication of the 3D graphene-based cubes involves: (i) preparation of protection layers, (ii) graphene-membrane transfer and patterning, (iii) metal surface patterning on graphene-membranes, (iv) frame and hinges patterning and deposition, (v) self-folding, and (vi) removal of the protection layers

(**Figure 1**). This article focuses mostly on the self-folding aspects of the 3D graphene-based cubes fabrication. Details on physical and optical properties of the 3D graphene-based cubes can be found in our other recent publications[27,28].

Protocol

CAUTION: Several of the chemicals used in these syntheses are toxic and may cause irritation and severe organ damage when touched or inhaled. Please use appropriate safety equipment and wear personal protective equipment when handling the chemicals.

1. Preparation of Aluminum Oxide and Chromium Protection Layers on a Copper Sacrificial Layer

1. Using an electron-beam evaporator, deposit 10 nm thick chromium (Cr) and 300 nm thick copper (Cu) layers (sacrificial layer) on the silicon (Si) substrate (**Figure 2a**).
2. Spin-coat a photoresist (PR)-1 at 2500 rpm followed by baking at 115 °C for 60 s.
3. Expose the designed 2D net areas to ultraviolet (UV) light on a contact mask aligner for 15 s and develop for 60 s in developer-1 solution. Rinse the sample with deionized (DI) water and blow-dry with an air gun.
4. Deposit 10 nm thick Cr layer and lift-off of the remaining PR-1in acetone. Rinse the sample with DI water and blow-dry with an air gun (**Figure 2b**).
5. To pattern 2D nets with six square Al_2O_3/Cr protection layers on the 2D net, spin-coat a PR-1 at 2500 rpm followed by baking at 115 °C for 60 s.
6. Expose the designed six square protection layers to UV light on a contact mask aligner for 15 s and develop for 60 s in developer-1 solution. Rinse the sample with DI water and blow-dry with an air gun.
7. Deposit a 100 nm thick Al_2O_3 layer and 10 nm thick Cr layer. Remove remaining PR-1in acetone. Rinse the sample with DI water and blow-dry with an air gun (**Figure 2c**).

2. Preparation of Graphene and Graphene Oxide Membranes

Note: In this study, two types of graphene-based materials are used: (i) chemical vapor deposition (CVD) grown graphene and (ii) graphene oxide (GO).

1. **Preparation of multilayer CVD graphene membranes**
   Note: To obtain multilayer graphene membranes, single-layer graphene is transferred three separate times using multiple polymethyl methacrylate (PMMA) coating/removal steps.
   1. Starting with a ~15 mm square piece of graphene adhered on Cu foil, spin-coat a thin PMMA layer at 3000 rpm on the surface of the graphene. Bake at 180 °C for 10 min.
   2. Place the PMMA/graphene/Cu foil-layered sheet floating Cu-side down in Cu etchant for 24 h to etch away the Cu foil.
   3. After the Cu foil is completely dissolved (leaving PMMA/graphene), transfer the floating PMMA-coated graphene onto the surface of a pool of DI water using a microscope slide glass to remove any Cu etchant residue. Repeat the transfer of the PMMA-coated graphene onto new DI water pools several times to adequately rinse.
   4. Transfer the floating PMMA-coated graphene onto another piece of graphene adhered on Cu foil (graphene/Cu) to obtain a bi-layer graphene membrane (forming a PMMA/graphene/graphene/Cu foil structure).
   5. Thermally treat the double-layer graphene on the Cu foil on a hot plate at 100 °C for 10 min.
   6. Remove the PMMA on top of the double-layer graphene on the Cu foil in an acetone bath (leaving a graphene/graphene/Cu foil layer stack), followed by transferring to DI water.
   7. Repeat the graphene transfer (2.1.1 - 2.1.5) one more time to get three stacked layers of graphene membranes. When step 2.1.4 is reached during the repeat process, instead of transferring the new PMMA-coated graphene sheet onto another piece of graphene/Cu, transfer the new PMMA-coated graphene onto the previously fabricated graphene double-layer from step 2.1.6 to form a PMMA/graphene/graphene/graphene/Cu foil layer combination. Then, repeat step 2.1.5 without modification.
   8. Place the PMMA/graphene/graphene/graphene/Cu foil-layered sheet floating Cu-side down in Cu etchant for 24 h to etch away the Cu foil.
   9. Transfer the PMMA-coated three-layers of graphene membranes (PMMA/graphene/graphene/graphene) onto the pre-fabricated Al_2O_3/Cr protection layers from section 1.
   10. After transfer of the graphene, remove the PMMA with acetone. Then, dip the sample in DI water and dry in air.
   11. Thermally treat the multi-layer graphene on the substrate on a hot plate at 100 °C for 1 h.
   12. Spin-coat PR-1 at 2500 rpm and bake at 115 ˚C for 60 s.
   13. UV expose the regions of PR-1 directly above the square protection layer areas using a contact mask aligner for 15 s and develop for 60 s in developer-1 solution.
   14. Remove the newly uncovered, unwanted graphene areas *via* an oxygen plasma treatment for 15 s.
   15. Remove the leftover PR-1 in acetone.
   16. Rinse the sample with DI water and dry in air (**Figure 2d**).

2. **Preparation of graphene oxide membranes**
   Note: Traditional photolithography followed by a lift-off process *via* flood exposure is used to pattern the GO membranes.
   1. Spin-coat PR-2 at 1700 rpm for 60 s on top of the previously fabricated Al_2O_3/Cr protection layers to obtain a 10 µm thick layer. Bake the PR-2 at 115 °C for 60 s and then wait for 3 h.
   2. With the same mask used for patterning the Al_2O_3/Cr protection layer, UV expose the sample on a contact mask aligner for 80 s and develop for 90 s in developer-2 solution. Rinse the sample with DI water and blow-dry with an air gun.

3. Perform a UV flood exposure of the entire sample without a mask for 80 s.
4. Spin-coat the prepared GO and water mixture (15 mg of GO powder in 15 mL of DI water) on the sample at 1000 rpm for 60 s. Perform the spin-coating a total of 3 times.
5. Dip the sample in developer-2 solution to allow lift-off of unwanted GO.
6. Rinse the sample with DI water and carefully blow-dry the sample with an air gun.
7. Thermally treat the sample on a hot plate at 100 °C for 1 h (**Figure 2h**).

3. Metal Surface Patterning on Graphene-Based Membranes

Note: A common photolithography process was conducted to achieve the surface patterning using a UV contact mask aligner and electron-beam evaporator (see 1.2 - 1.4).

1. Create 20 nm thick titanium (Ti) patterns on top of the patterned graphene-based membranes.
2. Thermally treat the sample on a hot plate at 100 °C for 1 h (**Figure 2e** for graphene and **Figure 2i** for GO).

4. Fabrication of Polymer Frames and Hinges

1. On top of graphene-based membranes with Ti surface patterns, spin-coat PR-3 at 2500 rpm for 60 s to form a 5 µm thick layer and bake at 90 °C for 2 min.
2. UV expose the samples for 20 s, bake at 90 °C for 3 min, and develop for 90 s in developer-3 solution.
3. Rinse the sample with DI water and isopropyl alcohol (IPA) and carefully blow-dry the sample with an air gun.
4. Post-bake the samples at 200 °C for 15 min to enhance the mechanical stiffness of the (PR-3) frames (**Figure 2f** for graphene and **Figure 2j** for GO).
5. To make the hinge pattern, spin-coat PR-2 at 1000 rpm for 60 s to form a 10 µm thick film on top of the prefabricated substrate. Bake at 115 ˚C for 60 s and wait for 3 h.
6. UV expose the sample on a contact mask aligner for 80 s and develop for 90 s in developer-2 solution.
7. Rinse the sample with DI water and carefully blow-dry the sample with an air gun (**Figure 2g** for graphene and **Figure 2k** for GO).

5. Self-Folding in DI Water

Note: When the PR-2 hinges are melted (or reflow), a surface tension force is generated; hence, the 2D structures transform into 3D structures (a self-folding process).

1. To release the 2D structure, dissolve the Cu sacrificial layer under the 2D nets in a Cu etchant (**Figure 2l**).
2. Carefully transfer the released structure into a DI water bath by using a pipet and rinse a few times to remove the residual Cu etchant.
3. Place the 2D structure in DI water heated above the melting point of the polymer (PR-2) hinges (**Figure 2m**).
4. Monitor the self-folding in real-time *via* optical microscopy and remove from the heat source on successful assembly into closed cubes.

6. Removal of the Protection Layers

1. After self-folding, remove the Al_2O_3/Cr protection layers with Cr etchant (**Figure 2n**).
2. Gently transfer the cubes into a DI water bath and carefully rinse.

Representative Results

Figure 2 displays optical images of the lithographic processes of the 2D graphene and GO net structures and subsequent self-folding process. The self-folding process is monitored in real-time *via* a high-resolution microscope. Both types of 3D graphene-based cubes are folded at ~80 °C. **Figure 3** lays out video captured sequences showing the self-folding of 3D graphene-based cubes in a parallel manner. Under an optimized process, this approach shows a highest yield of ~90%.

Figure 4 shows optical images of the 3D assembled graphene- and GO-based cubes with and without surface patterns. The overall size of the self-folded cubes is 200 (width) × 200 (length) × 200 (height) μm^3. To show the surface patterning ability, 20 nm thick Ti patterned features and "UMN" lettering are defined on each face of the 3D graphene-based cubes.

To evaluate the structural changes in the graphene and GO membranes during the self-folding process, properties of the graphene and GO structures before and after self-folding are characterized *via* Raman spectra. **Figure 5a and 5b** include Raman spectroscopy of pristine graphene-based materials, 2D graphene-based nets, and 3D graphene-based cubes. The results show no noticeable changes in Raman peak position and intensity for both graphene and GO membranes after the self-folding. However, when protection layers are not used (**Figure 5c**), noticeable changes in relative peak intensities were observed, indicating the changes or damages to the properties of graphene during the self-folding.

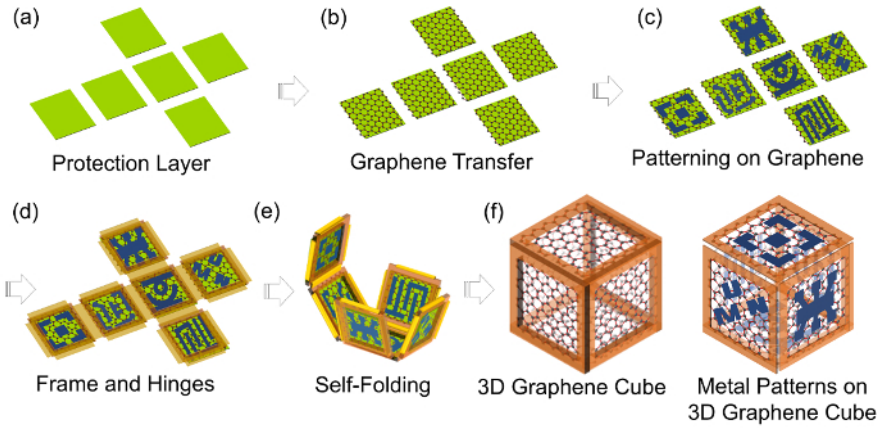

Figure 1: Schematic illustration of the self-folding process of 3D graphene-based cubes (a) patterning 2D net protection layer. (b) transferring graphene-based membranes on top of the protection layer. (c) metal surface patterning on graphene-based membranes. (d) patterning frame and hinge. (e) releasing the 2D structures from the substrate and self-folding driven by the reflow of the hinges *via* high temperature. (f) removal of the protection layer of 3D graphene-based cubes. This figure is adapted with permission[28]. Copyright 2017, American Chemical Society. Please click here to view a larger version of this figure.

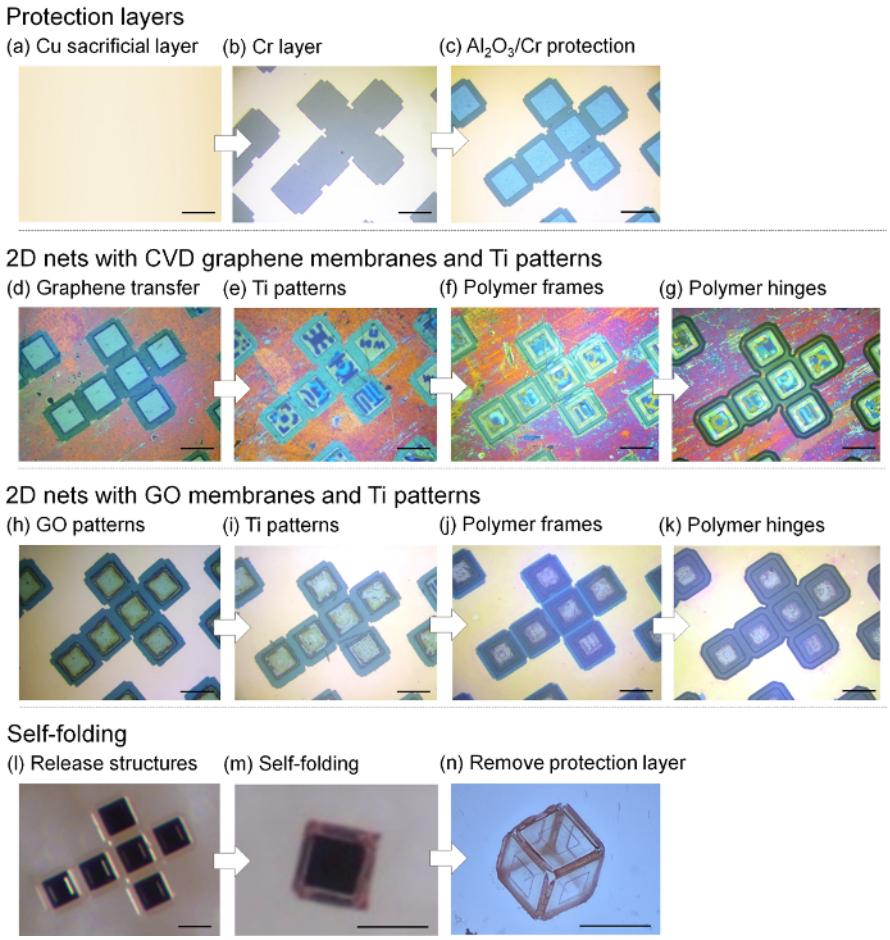

Figure 2: Optical images of the lithographic fabrication process of 2D graphene and GO net structures and subsequent self-folding process (a-c) Fabrication of protection layers. (a) 10 nm thick Cr and 300 nm thick Cu sacrificial layers are deposited on a Si wafer. (b) 10 nm thick Cr layer and (c) 100 nm thick Al_2O_3/10 nm thick Cr protection layers are defined (160 × 160 μm^2). **(d-g) 2D nets with CVD graphene membranes and Ti patterns.** (d) The multilayer graphene is transferred onto the substrate and patterned *via* an oxygen plasma treatment. (e) On top of the patterned graphene membranes, 20 nm thick Ti patterns are defined. (f) The 5 µm thick PR-3 frames are patterned. (g) To make the hinge pattern, a 10 µm thick PR-2 film is patterned. **(h-k) 2D nets with GO membranes and Ti patterns.** (h) GO in water is spin-coated three times at 1000 rpm for 60 seconds to produce ~10 nm thick GO membranes. A lift-off *via* flood exposure process is performed to pattern the GO membranes. (i) On top of the patterned GO, Ti patterns are defined. Then, (j) the PR-3 cubic frames and (k) PR-2 hinges are patterned. **(l-n) Self-folding process.** (l) Release of the 2D nets from the sacrificial layer. (m) Self-folding of the free-standing 2D nets in water by applying a temperature of ~80 °C. (n) Removal of the protection layers. Scale bar =200 µm. This Figure is adapted with permission[28]. Copyright 2017, American Chemical Society. Please click here to view a larger version of this figure.

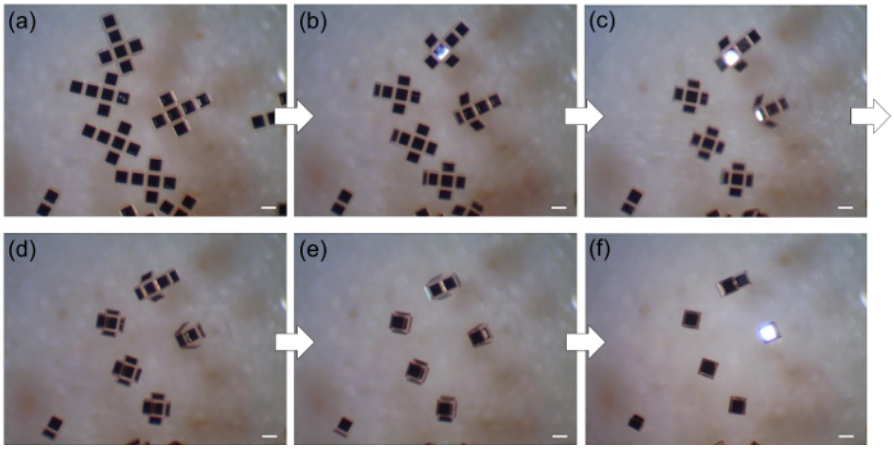

Figure 3: A video-captured sequence of the self-folding process of 3D graphene-based cubes Real-time optical images of 3D graphene-based cubes captured after (a) 0, (b) 30, (c) 60, (d) 90, (e) 120, and (f) 150 s (before etching the protection layer). Scale bar =200 μm. Please click here to view a larger version of this figure.

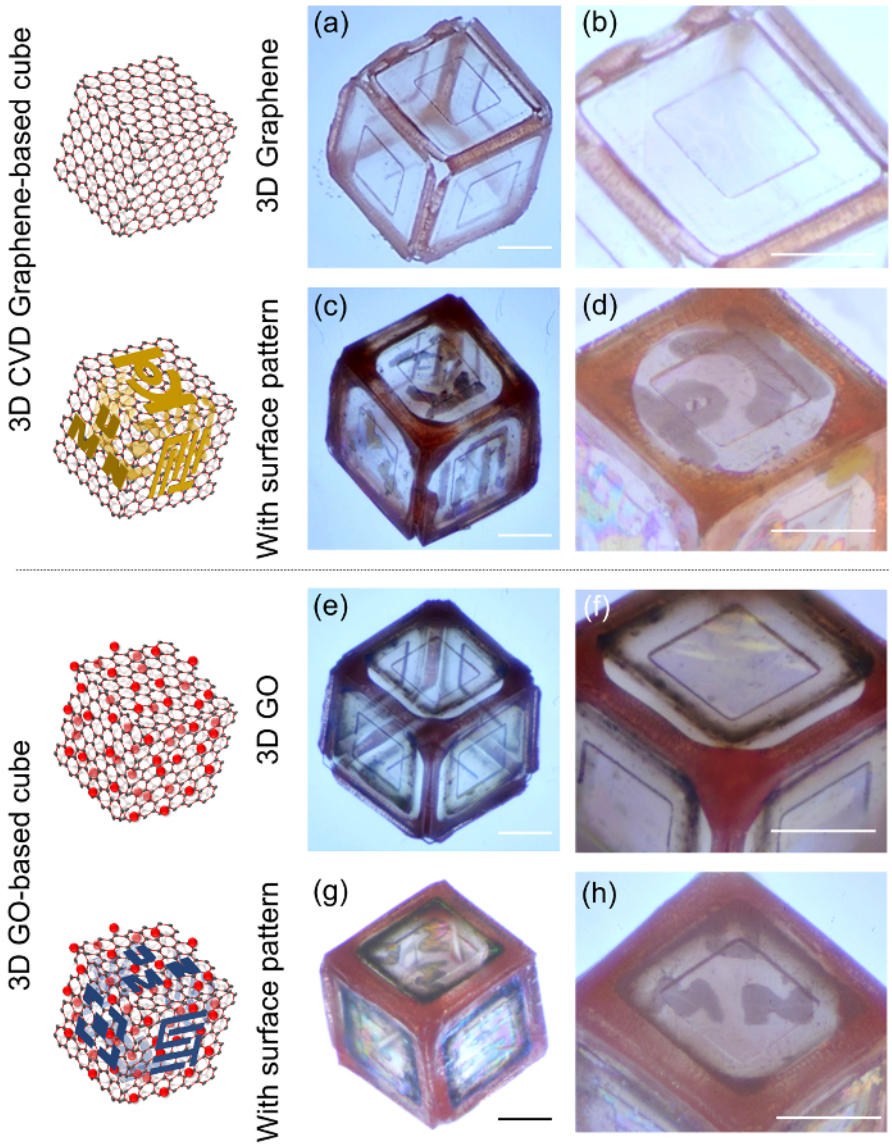

Figure 4: Optical images of the 3D graphene-based cubes with and without surface patterns (a-b) a 3D cube with three layers of CVD graphene films and a zoomed-in image of the top surface of the 3D CVD graphene-based cube. (c-d) a 3D cube with metal patterns (20 nm thick Ti) on the CVD graphene membranes and a zoomed-in image of the top surface of the 3D graphene-based cube with the Ti patterns. (e-f) a 3D GO-based cube and a zoomed-in image of the top surface of the 3D GO-based cube. (g-h) a self-folded 3D GO-based cube with Ti patterns and a zoomed-in image of the top surface of the 3D GO-based cube with the Ti patterns. Scale bar = 100 μm. This figure is adapted with permission[28]. Copyright 2017, American Chemical Society. Please click here to view a larger version of this figure.

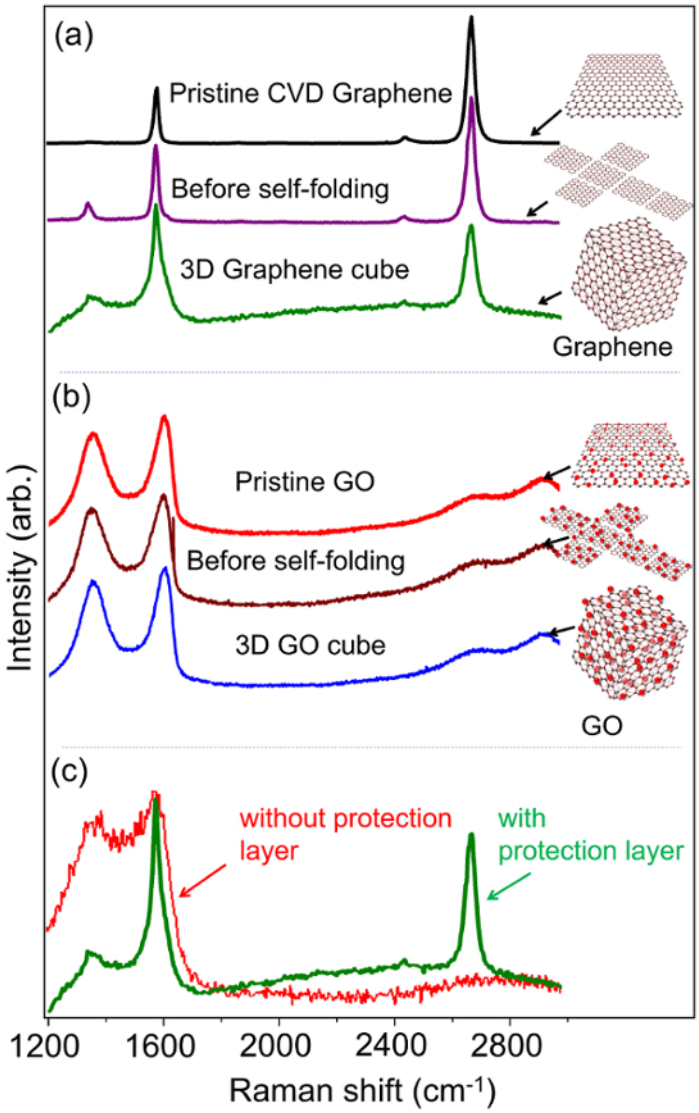

Figure 5: Raman spectroscopy of 2D graphene-based membranes and 3D graphene-based cubes (a) Raman spectrum of pristine CVD graphene on a Si substrate, 2D patterned CVD graphene (before self-folding), and free-standing 3D graphene cubes (after self-folding). The three peaks near ~ 1340 cm^{-1} (D band), ~ 1580 cm^{-1} (G band) and ~ 2690 cm^{-1} (2D band) are observed. (b) Raman spectrum of ~ 10 layers (~ 10 nm thick) of GO films on Si, before self-folding, and after self-folding (free-standing cubes). The four peaks at ~ 1360 cm^{-1} (D band), ~ 1605 cm^{-1} (G band), ~ 2715 cm^{-1}, and ~ 2950 cm^{-1} (D+G band) are observed. (c) Raman spectrum of 3D graphene-based structures with (green) and without (red) the use of the Al_2O_3/Cr protection layer. Please click here to view a larger version of this figure.

Discussion

For the cubes fabricated with CVD graphene, because each face of a given cube is designed with an outer frame surrounding a ~160 × 160 μm^2 area of free-standing graphene, a single sheet of monolayer graphene does not have the necessary strength to permit parallel processing of the cubes. For this reason, graphene membranes consisting of three layers of CVD graphene monolayer sheets are produced *via* three separate graphene transfers using multiple PMMA coating/removal steps. On the other hand, for GO membrane preparation, we use individual GO sheets in water, obtained *via* a modified Hummer's method[27].To pattern the GO membranes, traditional photolithography followed by a lift-off process *via* flood exposure is used. The process uses a flood exposure after traditional photolithography but before GO membrane deposition. After GO spin-coating, a lift-off process is then performed in developer to remove the unwanted GO areas. Some developers contain sodium hydroxide (NaOH) aqueous alkaline solution which etches aluminum and Al_2O_3. Therefore, a NaOH free developer should be used. For this work, the specific developer used to fulfill this requirement is developer-2 solution.

The frames of the 3D cubes supporting the graphene-based membranes are made of PR-3 due to its high mechanical and thermal stability as well as high optical transparency[29]. It is known that the thermal and mechanical stability of PR-3 depends on the cross-linking process[30]. The maximum cross-linking of PR-3 occurs when it is hard-baked over ~200 °C. After the hard-baking, the dynamic modulus of PR-3 improves, indicating that the structures have more mechanical strength during dynamic motion and thus are more mechanically stable. In fact, when the heat is applied to the cubes (or samples) for self-folding, the PR-3 frames maintain their original shape. Another source of potential damage is the deposition of Ti patterns as they might produce compressive stress on the graphene membranes; however, the demonstration of undamaged

graphene membranes after self-folding indirectly indicates the mechanical stability of the PR-3 could contribute to the conservation of the graphene membranes (**Figure 3, Figure 4**). Furthermore, the photo-definable property of PR-3 allows easy control of the sizes and shapes of the 3D cubes, along with easy control of the folding angle of 3D structures for the realization of diverse 3D structures including semi-3D structures.

In the origami-like self-folding principle, a surface tension torque is produced to fold a 2D net structure *via* the reflow of the hinge materials (*e.g.*, thin metal films or thermal-sensitive polymers)[26,31]. The surface tension of the polymer PR-2 hinges is lower (~0.03 N/m) than that of metal hinges (*e.g.,* solder ~0.5 N/m)[26,28]. The lower surface tension produces less rotational torque when the 2D nets are folded compared to 2D nets with metal hinges[26,31]. The lower torque could reduce the stress on the tri-layer graphene-based membranes during the self-folding process. The 3D graphene-based cubes are folded at ~80 °C (**Figure 3**), in which the hinges reflow at their melting point (for metal solder hinges, the melting point is ~230 °C)[26]. Remarkably, under an optimized process, this approach shows a highest yield of ~90%.

During the lithography process and self-folding, the spatial stress on graphene membranes induces delamination, buckling, cracking, and/or ripping. For example, (i) when the 2D nets with graphene membranes are released from the sacrificial layer, strong *Van der Waals* forces between the graphene and sacrificial layer (including Cu or even many other substrates) can be generated, resulting in broken graphene membranes; and (ii) during the self-folding in liquid, surface tension force, fluidic force, and gravitational force cause cracking and buckling of graphene membranes. A Cu layer is used for a sacrificial layer and an additional patterned Al_2O_3/Cr layer is used as a protection layer to shield the graphene-based membranes. Initially, a thin (10 nm thick) Cr layer has been used as a protection layer. However, the thin Cr layer shows buckling structures since the mechanical properties of the Cr layer are not strong enough to hold the graphene-based membranes when the structure is released from the Cu sacrificial layer. Later, to resolve this issue, 100 nm thick Al_2O_3/10 nm thick Cr layers are added on top of the 10 nm thick Cr/300 nm thick Cu sacrificial layer as described above. As a result, the protection layer allowed retention of the graphene membranes throughout the fabrication process and self- folding. The protection layers on the 3D cube can be removed after self-folding by an appropriate etchant without damage to the graphene membranes.

The 3D CVD graphene-based cube image presents a highly transparent, free-standing, enclosed architecture (**Figure 4a**) with no noticeable cracks, ripples, holes, or other damage on the membranes (from the zoomed-in image, **Figure 4b**). As described above, using the same approach used to produce the 3D CVD graphene-based cubes, we also successfully demonstrate the fabrication of cubes with membranes comprised of ~10 layers (~10 nm thick) of GO sheets (**Figure 4e, 4f**). In addition, Ti surface patterned 3D cubes are very stable (**Figure 4c, 4d** for graphene and **Figure 4g, 4h** for GO), and the demonstration of varied surface modifications with dissimilar designs on the different faces suggests a versatile strategy for the construction of 3D multifunctional devices with heterogeneous integration of different combinations of materials. As a result, the 3D graphene-based cubes show (i) free-standing CVD graphene and GO window membranes comprised of layered structures (no composite formation); (ii) enclosed but hollow structures that do not require an additional support or substrate; and (iii) surface modifications *via* metal patterning on the graphene or GO surfaces with any desired patterns, because our approach is compatible with conventional lithographic processes.

Raman spectroscopy is well-established as an effective, noninvasive method to characterize graphene and related materials, and it can supply a wide variety of details about graphene-based samples such as thickness, doping, disorder, edge and grain boundaries, thermal conductivity, and strain. Furthermore, this characterization method is flexible as it can be applied to a sample in various environmental conditions[32,33,34,35]. Therefore, if there are significant changes in the structure of graphene, we should be able to see changes in Raman peaks positions or intensities after self-folding. As shown in **Figure 5a-5b**, no significant changes in the peak positions and intensities can be seen after the self-folding, since the Al_2O_3/Cr protection layers help to shield the graphene-based membranes (both CVD graphene and GO) during fabrication. However, as shown in **Figure 5c**, when protection layers are not used, graphene membranes are damaged during the self-folding, resulting in a higher D band (~1340 cm^{-1}) and a lower 2D band (~2690 cm^{-1}). The quantitative information on the graphene defects can be analyzed by the peak intensity ratio of the D band and G band (I_D/I_G): low value I_D/I_G means low-defect graphene. From **Figure 5a** we calculate the I_D/I_G values of the 3D graphene to be ~0.65 which is comparable to other CVD graphene multilayer sheets[36]. Therefore, these observations indicate the self-folding process did not create significant changes in the CVD graphene and GO membranes (the materials retain their intrinsic properties, and no chemical intercalation between layers occurs), demonstrating the robustness of the reported method.

In addition to producing hollow, free-standing, polyhedral cubes, the self-folding method employed here allows for surface patterning, consisting of metal, insulator, and semiconductor materials on the 2D graphene membranes, to be applied to the cubes while maintaining the intrinsic properties of the graphene. This allows for the development of electronic and optical devices, including sensors and electric circuits, utilizing the numerous advantages of 3D configurations. Furthermore, since the processes used are not limited to only graphene-based materials, this method may be applied to other 2D materials such as transition metal dichalcogenides and black phosphorus, thereby allowing our fabrication approach to be harnessed in developing next-generation 3D reincarnations of 2D materials.

The high-temperature (~80 °C) required by the folding mechanism could be problematic in biomedical applications unless the process can be further optimized to reduce the folding temperature. Additionally, the PR-2 hinge material is not a biocompatible material. Future studies will focus on developing biocompatible hinge materials that respond at low-temperature (or low-energy) such as polyesters and synthetic hydrogels. We have recently been able to manufacture similar structures *via* a remote-controlled self-folding mechanism that could be useful in this respect[37].

Disclosures

The authors have nothing to disclose.

Acknowledgements

This material is based upon work supported by a start-up fund at the University of Minnesota, Twin Cities and an NSF CAREER Award (CMMI-1454293). Parts of this work were carried out in the Characterization Facility at the University of Minnesota, a member of the NSF-funded Materials Research Facilities Network (*via* the MRSEC program. Portions of this work were conducted in the Minnesota Nano Center, which

is supported by the National Science Foundation through the National Nano Coordinated Infrastructure Network (NNCI) under Award Number ECCS-1542202. C. D. acknowledges support from the 3M Science and Technology Fellowship.

References

1. Geim, A. K., & Novoselov, K. S. The rise of graphene. *Nature Materials.* **6**, (3), 183-191 (2007).
2. Singh, V. *et al.* Graphene based materials: Past, present and future. *Progress in Materials Science.* **56**, (8), 1178-1271 (2011).
3. Bonaccorso, F., Sun, Z., Hasan, T., & Ferrari, A. C. Graphene photonics and optoelectronics. *Nature Photonics.* **4**, (9), 611-622 (2010).
4. Wang, C., Li, D., Too, C. O., & Wallace, G. G. Electrochemical Properties of Graphene Paper Electrodes Used in Lithium Batteries. *Chemistry of Materials.* **21**, (13), 2604-2606 (2009).
5. Bunch, J. S. *et al.* Electromechanical resonators from graphene sheets. *Science.* **315**, (5811), 490-493 (2007).
6. Menaa, F., Abdelghani, A., & Menaa, B. Graphene nanomaterials as biocompatible and conductive scaffolds for stem cells: impact for tissue engineering and regenerative medicine. *Journal of Tissue Engineering and Regenerative Medicine.* **9**, (12), 1321-1338 (2015).
7. Han, M. Y., Özyilmaz, B., Zhang, Y., & Kim, P. Energy band-gap engineering of graphene nanoribbons. *Physical Review Letters.* **98**, (20), 206805 (2007).
8. Son, Y.-W., Cohen, M. L., & Louie, S. G. Half-metallic graphene nanoribbons. *Nature.* **444**, (7117), 347-349 (2006).
9. Yan, Q. *et al.* Intrinsic current− voltage characteristics of graphene nanoribbon transistors and effect of edge doping. *Nano Letters.* **7**, (6), 1469-1473 (2007).
10. Fei, Z. *et al.* Gate-tuning of graphene plasmons revealed by infrared nano-imaging. *Nature.* **487**, (7405), 82-85 (2012).
11. Joung, D., Zhai, L., & Khondaker, S. I. Coulomb blockade and hopping conduction in graphene quantum dots array. *Physical Review. B.* **83**, (11), 115323 (2011).
12. Bacon, M., Bradley, S. J., & Nann, T. Graphene quantum dots. *Particle & Particle Systems Characterization.* **31**, (4), 415-428 (2014).
13. Blees, M. K. *et al.* Graphene kirigami. *Nature.* **524**, (7564), 204-207 (2015).
14. Michael Cai, W. *et al.* Mechanical instability driven self-assembly and architecturing of 2D materials. *2D Materials.* **4**, (2), 022002 (2017).
15. Shenoy, V. B., & Gracias, D. H. Self-folding thin-film materials: From nanopolyhedra to graphene origami. *MRS Bulletin.* **37**, (9), 847-854 (2012).
16. Zhu, S., & Li, T. Hydrogenation-Assisted Graphene Origami and Its Application in Programmable Molecular Mass Uptake, Storage, and Release. *ACS Nano.* **8**, (3), 2864-2872 (2014).
17. Zhang, L., Zeng, X., & Wang, X. Programmable hydrogenation of graphene for novel nanocages. *Scientific Reports.* **3**, 3162 (2013).
18. Vickery, J. L., Patil, A. J., & Mann, S. Fabrication of Graphene-Polymer Nanocomposites With Higher-Order Three-Dimensional Architectures. *Advanced Materials.* **21**, (21), 2180-2184 (2009).
19. Yang, X., Zhu, J., Qiu, L., & Li, D. Bioinspired effective prevention of restacking in multilayered graphene films: towards the next generation of high-performance supercapacitors. *Advanced Materials.* **23**, (25), 2833-2838 (2011).
20. Choi, B. G., Yang, M., Hong, W. H., Choi, J. W., & Huh, Y. S. 3D macroporous graphene frameworks for supercapacitors with high energy and power densities. *ACS Nano.* **6**, (5), 4020-4028 (2012).
21. Niu, Z., Chen, J., Hng, H. H., Ma, J., & Chen, X. A leavening strategy to prepare reduced graphene oxide foams. *Advanced Materials.* **24**, (30), 4144-4150 (2012).
22. Li, Y. *et al.* Growth of conformal graphene cages on micrometre-sized silicon particles as stable battery anodes. *Nature Energy.* **1**, (2), 15029 (2016).
23. Cho, J. H., & Gracias, D. H. Self-Assembly of Lithographically Patterned Nanoparticles. *Nano Letters.* **9**, (12), 4049-4052 (2009).
24. Cho, J. H., Azam, A., & Gracias, D. H. Three Dimensional Nanofabrication Using Surface Forces. *Langmuir.* **26**, (21), 16534-16539 (2010).
25. Dai, C., & Cho, J. H. In Situ Monitored Self-Assembly of Three-Dimensional Polyhedral Nanostructures. *Nano Letters.* **16**, (6), 3655-3660 (2016).
26. Joung, D. *et al.* Self-Assembled Multifunctional 3D Microdevices. *Advanced Electronic Materials.* **2**, (6), 1500459 (2016).
27. Joung, D., Gu, T., & Cho, J. H. Tunable Optical Transparency in Self-Assembled Three-Dimensional Polyhedral Graphene Oxide. *ACS Nano.* **10**, (10), 9586-9594 (2016).
28. Joung, D. *et al.* Self-Assembled Three-Dimensional Graphene-Based Polyhedrons Inducing Volumetric Light Confinement. *Nano Letters.* **17**, (3), 1987-1994 (2017).
29. Lian, K., Ling, Z.-g., & Liu, C. Thermal stability of SU-8 fabricated microstructures as a function of photo initiator and exposure doses. *Proceedings of SPIE.* **4980**, 209 (2003).
30. Winterstein, T. *et al.* SU-8 electrothermal actuators: Optimization of fabrication and excitation for long-term use. *Micromachines.* **5**, (4), 1310-1322 (2014).
31. Syms, R. R. A., Yeatman, E. M., Bright, V. M., & Whitesides, G. M. Surface tension-powered self-assembly of microstructures - the state-of-the-art. *Journal of Microelectromechanical Systems.* **12**, (4), 387-417 (2003).
32. Xie, X. *et al.* Controlled fabrication of high-quality carbon nanoscrolls from monolayer graphene. *Nano Letters.* **9**, (7), 2565-2570 (2009).
33. Ferrari, A. C., & Basko, D. M. Raman spectroscopy as a versatile tool for studying the properties of graphene. *Nature Nanotechnology.* **8**, (4), 235-246 (2013).
34. Childres, I., Jauregui, L. A., Park, W., Cao, H., & Chen, Y. P. Raman spectroscopy of graphene and related materials. In *New developments in photon and materials research.*, Jang, J. I., Ed. Nova Science Publishers: Hauppauge NY (2013).
35. Polsen, E. S., McNerny, D. Q., Viswanath, B., Pattinson, S. W., & Hart, A. J. High-speed roll-to-roll manufacturing of graphene using a concentric tube CVD reactor. *Scientific Reports.* **5**, (2015).
36. Wu, T., Shen, H., Sun, L., You, J., & Yue, Z. Three step fabrication of graphene at low temperature by remote plasma enhanced chemical vapor deposition. *RSC Advances.* **3**, (24), 9544-9549 (2013).
37. Liu, C., Schauff, J., Joung, D., & Cho, J. H. Remotely controlled microscale 3D self-assembly using microwave energy. *Advanced Materials Technologies.* **2**, (8), 1700035 (2017).

